Journal of Radiotherapy in Practice

cambridge.org/jrp

Rotational effect and dosimetric impact: HDMLC vs 5-mm MLC leaf width in single isocenter multiple metastases radiosurgery with Brainlab Elements™

Carlos Daniel Venencia[1], José Alejandro Rojas-López[1,2], Rogelio Manuel Díaz Moreno[1] and Silvia Zunino[1]

[1]Instituto Zunino, Obispo Oro 423, 5000, Córdoba, Argentina and [2]Universidad Nacional de Córdoba, 5000, Córdoba, Argentina

Original Article

Cite this article: Venencia CD, Rojas-López JA, Díaz Moreno RM, and Zunino S. (2023) Rotational effect and dosimetric impact: HDMLC vs 5-mm MLC leaf width in single isocenter multiple metastases radiosurgery with Brainlab Elements™. *Journal of Radiotherapy in Practice*. **22**(e35), 1–11. doi: 10.1017/S1460396922000048

Received: 6 December 2021
Revised: 12 January 2022
Accepted: 17 January 2022

Key words:
genetic algorithm; multiple metastases; MLC; radiosurgery

Author for correspondence:
Instituto Zunino, Obispo Oro 423, 5000, Córdoba, Argentina.
E-mail: alexrojas@ciencias.unam.mx

Abstract

Purpose: To analyse the impact of multileaf collimator (MLC) leaf width in multiple metastases radiosurgery (SRS) considering the target distance to isocenter and rotational displacements.
Methods: Ten plans were optimised. The plans were created with Elements Multiple Mets SRS v2·0 (Brainlab AG, Munchen, Germany). The mean number of metastases per plan was 5 ± 2 [min 3, max 9], and the mean volume of gross tumour volume (GTV) was 1·1 ± 1·3 cc [min 0·02, max 5·1]. Planning target volume margin criterion was based on GTV-isocenter distance and target dimensions. Plans were performed using 6 MV with high-definition MLC (HDMLC) and reoptimised using 5-mm MLC (MLC-5). Plans were compared using Paddick conformity index (PCI), gradient index, monitor units , volume receiving half of prescription isodose (PIV_{50}), maximum dose to brainstem, optic chiasm and optic nerves, and V12Gy, V10Gy and V5Gy for healthy brain were analysed. The maximum displacement due to rotational combinations was optimised by a genetic algorithm for both plans. Plans were reoptimised and compared using optimised margin.
Results: HDMLC plans had better conformity and higher dose falloff than MLC-5 plans. Dosimetric differences were statistically significant ($p < 0{\cdot}05$). The smaller the lesion volume, the higher the dosimetric differences between both plans. The effect of rotational displacements produced for each target in SRS was not dependent on the MLC ($p > 0{\cdot}05$).
Conclusions: The finer HDMLC offers dosimetric advantages compared with the MLC-5 in terms of target conformity and dose to the surrounding organs at risk. However, only dose falloff differences due to rotations depend on MLC.

Introduction

The introduction of the multileaf collimator (MLC) has incorporated new features to radiotherapy, enabling the generation of irregular field shapes and to modify them easily, the intensity modulation of fixed beams and the generation of volumetric modulation as from arcs. This allows improvements in conformity and homogeneity of the dose distribution.[1–5]

A study with intensity-modulated radiotherapy demonstrated that the use of finer MLC leaf would be clinically beneficial in cases involving very small or irregular target volumes.[5] The impact of the narrower leaf on radiotherapy treatment planning has been studied by many authors.[6–13] The impact of the MLC leaf width on stereotactic radiosurgery (SRS) and 3D conformal radiotherapy treatment plans was analysed for finer (1·7-mm and 3-mm) and wider (10-mm) MLC. The finer MLC allowed to comply with the Radiation Therapy Oncology Group (RTOG) treatment planning guidelines for SRS.[14] More recently, Wu et al. performed a dosimetric comparison between 2·5-mm and 5-mm MLC for SRS.[15] They demonstrated small dosimetric benefits of the finer MLC.[15] The state of art of MLC on SRS suggests that the finer MLC seems to be a promising approach on multiple metastases treatments.[15–24]

The use of a single isocenter in multiple metastases SRS (SIMM-SRS) treatment is widely used, and it has shown many advantages in comparison to multiple isocenter technique such as the reduction of treatment time, monitor units (MU) and setup uncertainties.[6,25]

SRS requires high-dose delivery, high-dose gradient and sub-millimetre precision. It is necessary to quantify the sources of uncertainty involved in the SRS treatment given its special characteristics. The mechanical uncertainties, for all the axes of the linear accelerators with gantry, can be quantified by means of the WL test according to the AAPM TG-142.[26] The mechanical precision for SRS is required to be less than 1 mm.[27] In the specific case of SIMM-SRS, the WL test might be not sufficient to ensure precision in all targets.[28] In addition, inasmuch as there is

© The Author(s), 2022. Published by Cambridge University Press.

no consensus on specific quality controls to determine the geometric precision in SIMM-SRS, it is of utmost importance to analyse the impact of the patient's setup, above all in single fraction treatments.

The study of the patient's setup uncertainties entails the dose degradation applying rotations and translations to the targets and the subsequent variation of the quality parameters: Paddick conformity index and the gradient index. There are few studies evaluating the geometric and dosimetric impact of MLC in SIMM-SRS treatments.[4,24] Until today, there are not enough studies related to the dosimetric impact of MLC and the associated setup uncertainties.[25,29,30] This evaluation is treatment technique-dependent. For volumetric arc radiotherapy (VMAT)[29], there are not the same considerations as for dynamic conformal arc (DCA) approach. VMAT optimises the dynamic MLC, gantry speed and dose rate. For DCA, the MLC shapes around the planning target volumes (PTVs) and as gantry rotates the aperture changes according to the beam eye view of the PTV. Every 1 to 10 degrees static open projection of PTV changes. The comparison between VMAT and DCA was evaluated in the work of Molinier et al. for multiple metastases SRS.[31] The VMAT plans were more appropriate than the DCA due to the conformity and homogeneity of the dose distribution and the reduction of treatment time. However, for DCA the dose to the healthy brain is lower than for VMAT.[31]

In this work, the dosimetric impact of high-definition MLC (HDMLC) and 5-mm MLC (MLC-5) leaves was studied for SIMM-SRS by DCA technique using Elements™ Multiple Mets (Brainlab AG, Munchen, Germany) treatment planning system (TPS) taking into account the dose conformity, MU and the avoidance of healthy structures. Additionally, dosimetric differences due to rotation-induced displacements were studied for both MLC following the previous study of our work group.[32]

Method and Materials

Plan selection

Ten multiple brain metastases plan (55 metastases in total) were selected retrospectively. The average number of metastases was 5 ± 2 [min 3, max 10] per plan with an average gross tumour volume (GTV) volume of 1·1 ± 1·3 cc [min 0·02 cc, max 5·1 cc]. The prescribed dose to PTV volume was 21 Gy to D95%.

Patients were immobilised with SRS thermoplastic mask. A high-resolution (1 mm slice thickness) CT scan was acquired on a CT simulator (Somatom Spirit, Siemens Healthineers, Germany). T1, T2 and T1-weighted post-contrast magnetic resonance (MR) images (1 mm slice thickness, 1 mm spacing) were fused with CT images. The images were transferred to the TPS (Brainlab Elements, Brainlab AG, Munchen, Germany) for co-registration. All fusions were inspected and approved by the radiation oncologist. Organs at risk (OARs) were contoured by a physicist or dosimetrist (approved by a radiation oncologist) including the brain, chiasm, optic nerves, optic tract, eyes, lens, cochlea, brainstem and healthy brain. The healthy brain was defined as the volume of the brain minus the volumes of the GTVs and the brainstem. The GTV was delineated by the radiation oncologist and was equal to the clinical target volume (CTV).

The PTV was created following an institutional geometric margin criterion based on Kuntz et al. and others.[6,32–35] If the GTV is located less than 50 mm from the isocenter, a margin of 0·5 mm was assigned. If the GTV is located more than 50 mm from the isocenter or its volume was less than 0·1 cc, a margin of 1 mm was assigned.[32]

Treatment planning

Elements™ Multiple Mets SRS v2·0 (Brainlab AG, Munchen, Germany) is a commercial TPS that automatically optimises a dedicated set of dynamic arcs to treat single isocenter brain lesions.[36,37] The beams of the Elements™ plans were selected from a predefined template with 5 table angles. Both templates were defined following the institutional protocol. Treatment machine and the collimation system were selected as part of the planning process. The isocenter was selected automatically by the TPS, considering the average of the centre of mass of all GTVs.

SIMM-SRS plans were optimised for TrueBeam STx® using 6 MV beam with a flattening filter. HDMLC and MLC-5 were employed for planning. Both collimation systems are 120-leaf MLC with 60 central 2·5 mm leaves for HDMLC[38–40] and 5-mm leaves for MLC-5. The plans were optimised using the HDMLC and MLC-5, as shown in Figure 1. Dose calculation was performed with a 1 mm grid using the Brainlab pencil beam algorithm.[41–43] The plans were created using a dose template for a single fraction of 21 Gy with a desired PTV coverage of 95% and a tolerated coverage of 90%. The templates were set to aim a homogeneous dose distribution within the PTV. The quality index obtained from Elements™ report Paddick conformity index (PCI), gradient index (GI) and maximum dose (defined as the calculated maximum dose in the voxels) for the GTVs are shown in Table 1.

The MLC transmission factor and dosimetric leaf gap for the HDMLC were 1·23% and 0·86 mm,[44] respectively, and for the MLC-5 were 1·4% and 0·9 mm, respectively. These parameters were used in the machine profile configuration of Elements™ for TrueBeam STx®.

Dosimetric parameters such as Paddick conformity index (PCI),[45] gradient index (GI)[46] MU, volume receiving half of prescription isodose, maximum dose to brainstem, chiasm, cochlea, optic tract and optic nerves and the volume of 12 Gy, 10 Gy and 5 Gy to the healthy brain (V_{12}, V_{10} and V_5, respectively) were analysed. The PCI and GI were calculated based on the formal definition of those indices.[46–48] The PCI was calculated as shown in Equation 1:

$$PCI = \frac{TV^2_{PIV_{100}}}{TV \times PIV_{100}}, \quad (1)$$

where TV is the volume of the PTV, PIV_{100} is the volume of the prescription isodose, and $TV_{PIV_{100}}$ is the volume of the PTV covered by the prescription isodose. PIV_{50} is the volume of the 50% prescription isodose. The GI was calculated as shown in Equation 2:

$$GI = \frac{PIV_{50}}{PIV_{100}}. \quad (2)$$

Rotation-induced displacements

The impact of rotation-induced displacements was analysed for HDMLC and MLC-5 plans. At present, the commercial TPS could perform exclusively displacements (translations) on the planning structures to determine their dosimetric effect on targets and OARs. Rotations were not included in TPS. In a previous work[32],

https://doi.org/10.1017/S1460396922000048 Published online by Cambridge University Press

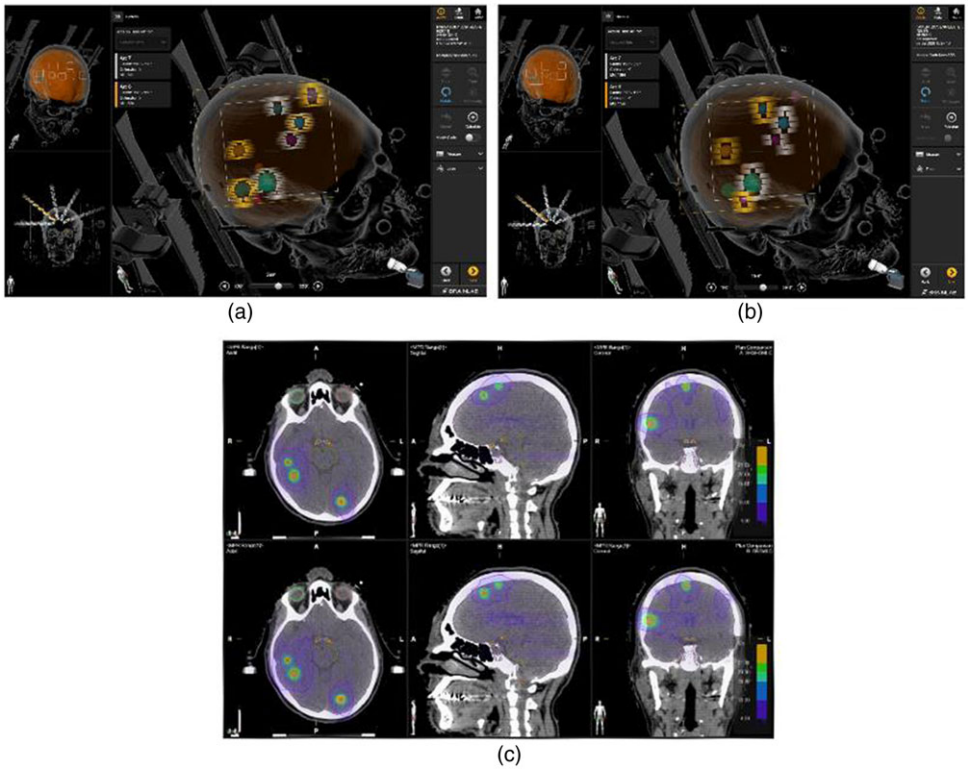


Figure 1. Comparison for a single isocenter multiple metastases radiosurgery (SIMM-SRS) plan for nine metastases between different multileaf collimator (MLC) leaf widths in Brainlab Elements: a) using HDMLC and b) using MLC-5. c) The dose distribution for both plans is compared between HDMLC (superior) and MLC-5 (inferior).

we worked out on the DICOM files handling to perform rotations of the targets with respect to a single point (isocenter). Additionally, it is known that the group of rotation transformations is non-commutative. The final location where the target was displaced depended on the rotational order and direction. Thus, the optimal combination of rotations is necessary to determine the maximum displacement produced. The complete study of rotational combinations implies to analyse mathematically all possible combinations by the product of the rotation matrices represented in Equation 3. To simplify the computations, the use of optimisation algorithms is useful in these cases considering the coded-uncoded information in bidimensional binary arrays. Bio-inspired optimisation algorithms such as genetic algorithm are easy to implement, they are robust and the optimal solution converged in few cycles.

$$R_{roll}(\theta) = \begin{pmatrix} 1 & amp;0 & amp;0 \\ 0 & amp;\cos\theta & amp;-\sin\theta \\ 0 & amp;\sin\theta & amp;\cos\theta \end{pmatrix}$$
$$R_{pitch}(\theta) = \begin{pmatrix} \cos\theta & amp;0 & amp;\sin\theta \\ 0 & amp;1 & amp;0 \\ -\sin\theta & amp;0 & amp;\cos\theta \end{pmatrix} \quad (3)$$
$$R_{yaw}(\theta) = \begin{pmatrix} \cos\theta & amp;-\sin\theta & amp;0 \\ \sin\theta & amp;\cos\theta & amp;0 \\ 0 & amp;0 & amp;1 \end{pmatrix}$$

The order and direction of rotations of 0·5º and 1º of each target were optimised and performed in three directions (roll, pitch and yaw) by the use of a genetic algorithm (GA) using in-house software. The software technical description is shown in literature.[32] It works under the assumption that if displacements are relatively small with respect to the relevant anatomical dimensions and the radiological path of the treatment beams towards the targets, this approach is valid for an arc treatment.[12] It allows to handle each structure from the DICOM structure file, applying rotations in any direction with respect to isocenter plan, while the CT and dose DICOM files remained fixed to display dosimetric calculations.

The rotational combinations were performed following the maximum displacement evaluated by a GA. The algorithm worked following the Darwinian principle of natural evolution and the DNA recombination process to reproduce naturally evolution processes and survival of the fittest to find the near-optimal solution.[49] In last years, the GA was implemented successfully in population pharmacokinetic models,[49] in multi-population for flexible job scheduling problem,[50] ensemble method for cancerous gene identification,[51] medical disease estimation,[52] protein design structure[53] and so on. The typical representation of GA is as follows: First, a random initial population of solutions represented as binary vectors (chromosomes) is generated. The first allele is defined for $j \leq 3$. Elements were transformed from the binary to the decimal system. There were 8 combinations in total for the first allele, and each one was assigned a particular combination of the order in which the couch rotations were performed. The second allele is defined for $j \geq 4$. Elements correspond to the rotational direction. If the gene is 1, the direction is clockwise (CW). Otherwise, if is 0, it is counterclockwise (CCW).[32] Second, the chromosomes were evaluated by the module of the difference vector between the centre of mass of the original structure and the displaced structure. Third, the best chromosomes were recombined in pairs by a cross-over point and two daughters were

https://doi.org/10.1017/S1460396922000048 Published online by Cambridge University Press

Table 1. GTV lesions and mean value and [min, max] of dosimetric parameters reported by the TPS for high-definition multileaf collimator (HDMLC) and **MLC**-5 plans

Plan	Number of metastases	GTV volume [cc]	HDMLC				MLC-5			
			D_{max} [Gy]	D_{min} [Gy]	PCI	GI	D_{max} [Gy]	D_{min} [Gy]	PCI	GI
1	6	0·70 [0·02, 3,60]	26·6 [23·91, 30·18]	18·06 [15·44, 19·22]	0·77 [0·66, 0·84]	5·20 [4·27, 6·62]	25·8 [24·17, 29·06]	18·41 [17·02, 19·25]	0·74 [0·61, 0·85]	6·55 [5·50, 7·20]
2	4	1·13 [0·22, 2·42]	24·19 [23·82, 24·68]	18·87 [18·13, 19·27]	0·82 [0·78, 0·87]	3·97 [3·15, 4·87]	24·16 [23·94, 24·54]	18·94 [18·25, 19·47]	0·83 [0·78, 0·87]	4·34 [3·47, 5·40]
3	5	0·92 [0·37, 2·88]	24·53 [23·64, 25·54]	18·53 [17·26, 19·57]	0·84 [0·82, 0·87]	4·10 [3·07, 4·74]	24·03 [22·95, 24·72]	18·64 [17·19, 19·86]	0·83 [17·19, 19·86]	4·59 [3·48, 5·81]
4	5	0·73 [0·11, 2·14]	24·07 [23·52, 25·01]	18·81 [17·41, 19·54]	0·80 [0·76, 0·84]	4·95 [3·31, 5·94]	23·71 [23·11, 24·22]	18·84 [17·50, 19·68]	0·80 [0·75, 0·84]	5·53 [3·63, 7·80]
5	3	2·79 [1·23, 5·07]	24·18 [23·85, 24·56]	17·61 [17·10, 18·60]	0·84 [0·82, 0·84]	3·32 [3·19, 3·47]	23·71 [23·39, 23·91]	18·12 [17·79, 18·53]	0·83 [0·81, 0·85]	3·64 [3·46, 3·92]
6	8	0·44 [0·02, 2·29]	25·61 [24·08, 27,75]	18·30 [17·50, 19·54]	0·79 [0·69, 0·84]	5·79 [5·51, 6·07]	22·71 [22·12, 23·71]	18·18 [16·46, 19·45]	0·77 [0·58, 0·85]	6·54 [5·91, 7·18]
7	10	0·48 [0·03, 2·27]	24·69 [23·67, 25·81]	18·69 [16·63, 19·42]	0·85 [0·75, 0·89]	4·88 [3·50, 6·46]	24·40 [22·84, 25·65]	18·91 [17·14, 19·93]	0·82 [0·75, 0·88]	5·61 [4·45, 6·71]
8	3	2·22 [0·63, 5·03]	24·44 [23·55, 25·55]	17·94 [17·29, 18·77]	0·86 [0·81, 0·89]	3·52 [3·48, 3·56]	23·76 [23·27, 24·21]	18·44 [18·18, 18,89]	0·84 [0·81, 0·87]	3·98 [3·58, 4·40]
9	4	0·62 [0·06, 1·45]	24·18 [23·36, 25·01]	18·65 [17·93, 19·30]	0·86 [0·82, 0·88]	4·94 [3·53, 6·97]	23·96 [23·12, 24·97]	19·18 [18·82, 19·60]	0·83 [0·77, 0·88]	5·55 [3·84, 7·46]
10	8	0,17 [0,07, 0·32]	24·10 [23·25, 24·73]	19·13 [18,09, 19·96]	0·85 [0·81, 0·88]	5·48 [4·49, 7·10]	23·96 [22·84, 24·80]	19·13 [18·03, 20·13]	0·81 [0·78, 0·85]	6·27 [5·03, 7·93]

generated. Fourth, the parents and daughters were subject to random bit mutations. Finally, the new chromosomes were evaluated. The process was iterative.

Dosimetric differences in PCI and GI were evaluated for the plans with non-rotated and rotated structures for each MLC leaf configuration.

Ethical Considerations

The treatment plans were selected and anonymised. There was no relationship between the plan and the personal data of the patients. The Institutional Quality Committee (Comité de Calidad Institucional) from our institution approved and authorised the use of this information, the results and the ethical conduct of this study.

Results

The dosimetric differences in terms of the MLC by the SRS-SIMM plans are shown in Figures 2 and 3. PCI and GI for HDMLC are higher than MLC-5 plans as shown in Table 2. In all cases, dosimetric differences are statistically significant ($p < 0{\cdot}05$). The p-values are shown in Table 1. The mean MU for HDMLC plans was 7528 ± 2180 MU [min 5418 MU, max 12,258 MU] and for MLC-5 plans was 7575 ± 2218 MU [min 4993 MU, max 11,673 MU]. The dosimetric differences between both plans tended to decrease as the lesion volume increased as represented by Pearson's coefficient for PCI ($r = -0{\cdot}1$ for HDMLC and $r = -0{\cdot}05$ for MLC-5) and for GI ($r = -0{\cdot}6$ for HDMLC and $r = -0{\cdot}6$ for MLC-5). In Figures 2 and 3 are shown the smaller lesion volume, the higher dosimetric differences between both plans. In addition to the lesion volume, the irregular shape of the metastases has an important role on the dosimetric impact considering different MLC, as shown in Figures 2 and 3 for the 5·3 cc lesion.

In Figures 2 and 3 are shown the data curve fitted only for visual guide, and the prediction levels were based on the existing fit to the data, and they were simultaneous for all predictor values. The simultaneous level measured the confidence that a new observation lies within 95% regardless of the predictor value. The fit is a single-term exponential to generated data and the bounds reflect a 95% confidence level. The intervals associated with a new observation are wider than the fitted function intervals because of the additional uncertainty in predicting a new response value (the curve plus random errors).

The use of HDMLC in an SRS-SIMM shows a remarkable reduction of the volume of 12 Gy, 10 Gy and 5 Gy to the healthy brain (V_{12}, V_{10} and V_5, respectively) with respect to MLC-5, as shown in Figure 4. It is shown that complying with the dose-volume constraints for both plans, there is an improvement on the reduction of organs at risk (optic nerves, optic tract, chiasm, cochlea and lens) maximum dose in all cases.

The degradation of the plans was evaluated by the dosimetric differences. The differences considered as $\left(X_{original} - X_{rotated}\right)/X_{original} \times 100$, where X is the dosimetric parameter (PCI or GI), were determined for both MLC leaf width plans. The differences between MLCs were no statistically significant $p = 0{\cdot}364$ for PCI and $p = 0{\cdot}762$ for GI by a two-tailed t-test.

To consider the GTV-to-PTV geometrical margin criterion used in this work, the dosimetric differences as a function of lesion volume and the maximum effective displacements produced by

https://doi.org/10.1017/S1460396922000048 Published online by Cambridge University Press

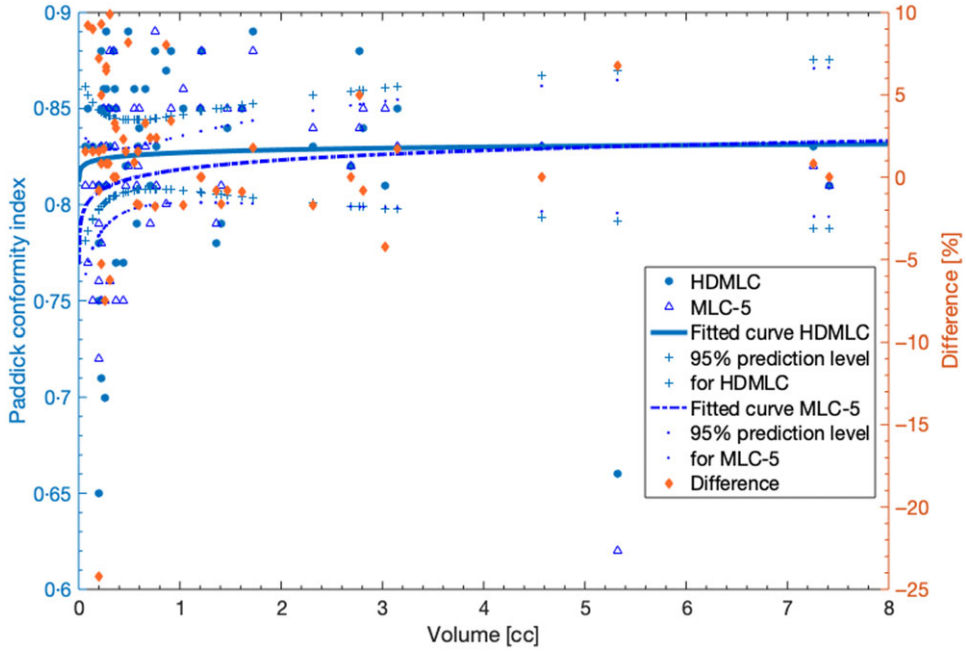


Figure 2. Left y-axis: Distribution of Paddick conformity index (PCI) as function of target volume for both plans using high-definition multileaf collimator HDMLC (blue circles) and MLC-5 (blue triangles). Solid and dashed lines represent the fitted curves for PCI as function of volume. The prediction functional levels of 95% are shown in dots for both plans. Right y-axis: Difference between two MLCs taken as reference HDMLC.

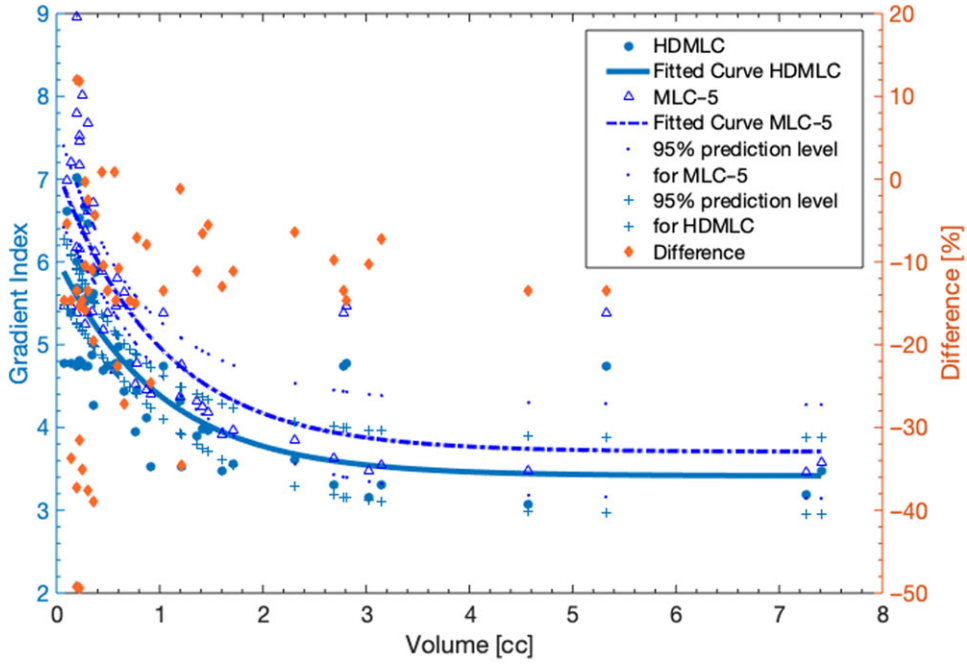


Figure 3. Left y-axis: Distribution of gradient index (GI) as function of target volume for both plans using high-definition multileaf collimator HDMLC (blue circles) and MLC-5 (blue triangles). Solid and dashed lines represent the fitted curves for PCI as function of volume. The prediction functional levels of 95% are shown in dots for both plans. Right y-axis: Difference between two MLCs taken as reference HDMLC.

rotations in three directions for 0·5° and 1° in each target are shown in Figures 5 and 6. The correlation between dosimetric differences, lesion volume and displacements were analysed. The Pearson correlation coefficient for all parameters is shown in Figures 7 and 8 for PCI and GI, respectively. There is no correlation between volume and dosimetric differences produced by rotations (ρ <0.08 for PCI and ρ <0.09 for GI); however, medium negative correlation ($\rho = -0.43$ for PCI and $\rho = -0.48$ for GI) was determined between displacements and dosimetric differences. In the case for rotation-induced displacement effect and MLC, the dosimetric differences were studied. Small positive correlation was determined for PCI ($\rho = 0.25$) and high positive correlation for GI ($\rho = 0.62$). Nevertheless, in all cases the higher dose difference, the higher maximum effective displacement up to 2 mm.

https://doi.org/10.1017/S1460396922000048 Published online by Cambridge University Press

Table 2. *Mean value, standard deviation and [min, max] of dosimetric parameters D_{99}, Paddick conformity index (PCI), gradient index (GI), volume receiving half of prescription isodose (PIV_{50}) and D_{max} for organs at risk for plans using high-definition multileaf collimator (HDMLC) and* ***MLC-5****. The p-values from one-tailed t-test are shown*

	HDMLC	MLC-5	*p*
D_{99} [Gy]	20·6 ± 0·5 [20·0, 24·3]	20·5 ± 0·8 [17·0, 22·5]	0·02
PCI	0·83 ± 0·05 [0·65, 0·89]	0·81 ± 0·04 [0·62, 0·89]	0·009
GI	5·0 ± 1·0 [3·1, 7·0]	6·0 ± 1·0 [3·5, 8·9]	6×10^{-8}
PIV_{50}	18·0 ± 4·0 [11·2, 25·5]	22·0 ± 6·0 [14·4, 29·8]	0·0002
Chiasm D_{max} [Gy]	1·6 ± 0·5 [1·0, 3·4]	1·8 ± 0·5 [1·3, 4·0]	0·01
Cochlea D_{max} [Gy]	1·6 ± 0·9 [0·6, 3·1]	1·8 ± 0·9 [0·8, 3·3]	0·004
Optic Nerves D_{max} [Gy]	1·3 ± 0·6 [0·7, 3·1]	1·4 ± 0·6 [0·8, 3·1]	0·04
Optic Tracts D_{max} [Gy]	2·0 ± 0·5 [1·7, 4·0]	2·3 ± 0·7 [1·8, 5·0]	0·02

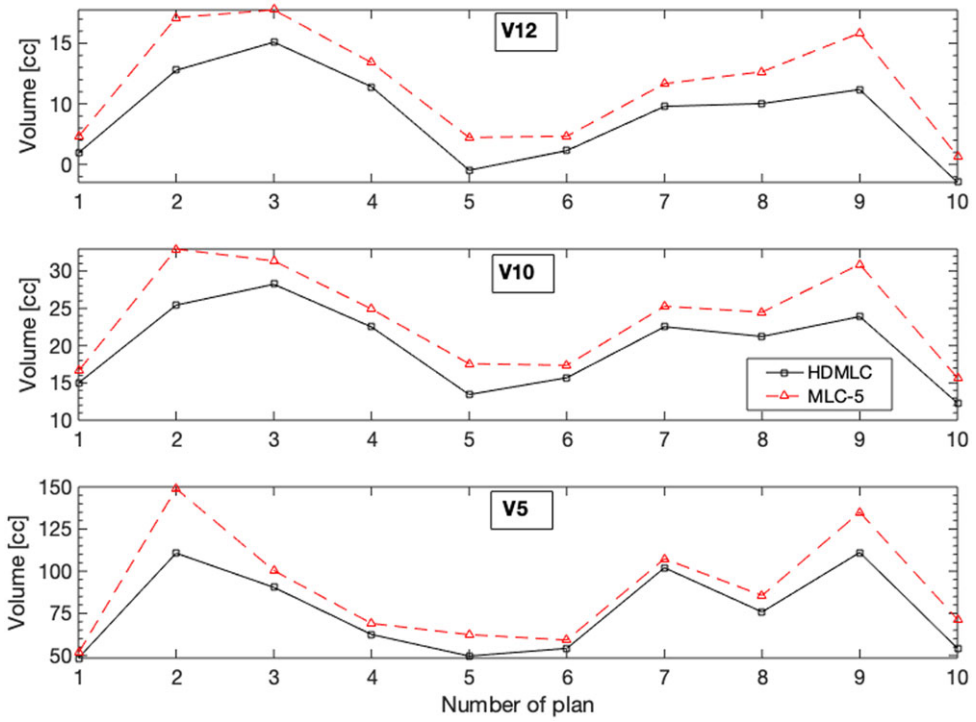


Figure 4. Dosimetric differences in healthy brain considering the volume that received 12 Gy, 10 Gy and 5 Gy (V_{12}, V_{10} and V_5, respectively) between the plans using high-definition multileaf collimator (HDMLC) and MLC-5.

Discussion

There was a statistically significant decrease in the PCI and GI for the HDMLC compared with MLC-5 ($p = 0{\cdot}09$ and 6×10^{-8}, respectively). These results are in concordance with other authors where they compared the Varian MLC and the micro-MLC for single targets.[17] The PCI difference between the MLCs ranged between 9·9% and 24·2% and the HDMLC exhibited better dose conformation as Tanyi et al. reported[22] indicating a worse conformity of the prescription isodose to the PTV using a wider MLC. Equivalent PTV coverage was achieved using the MLC-5 by adjusting the MLC shape around the target in every case. The GI differences between the two MLCs were higher, ranging from 0·8% to 49·2%. The higher differences were associated with smaller volume lesion (<0·3 cc) indicating a better dose falloff to the PTV using a HDMLC.

The indices in all cases were within some authors[15,53,54] and our institutional clinical criterion in the range from 0·65 to 0·9 to PCI and from 3·0 to 8·0 to GI. The MU between both plans has no difference in all ranges differing from what previous authors have reported.[17]

Small targets and complex geometrical distribution between OARs and targets are improved from the use of a finer MLC.[15] The HDMLC enhances PTV conformity and surrounding tissue sparing when compared to that of SMLC.[17] This advantage decreases when the target volume increases.

As other authors mentioned, the finer MLC yields dosimetric advantages in terms of target conformity and dose to the surrounding normal tissues.[18,55,56] The current study shows dosimetric benefits of the HDMLC over the MLC-5 for SRS multiple

https://doi.org/10.1017/S1460396922000048 Published online by Cambridge University Press

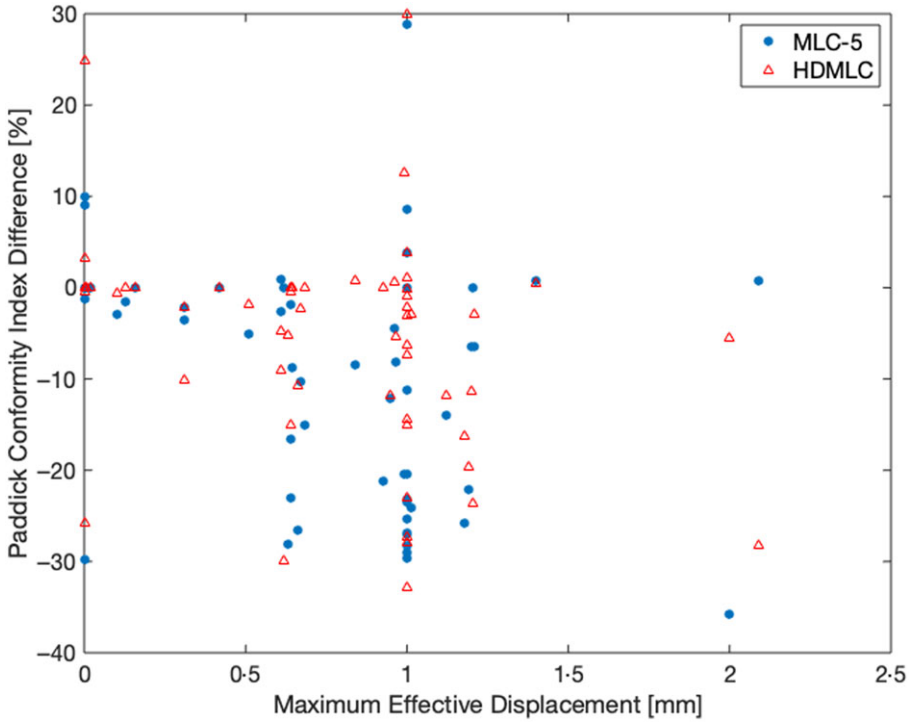


Figure 5. Comparison of the dosimetric difference produced between rotated and original plans for Paddick conformity index (PCI) between the target located in the original position (original) and the displaced (rotated) for HDMLC (red triangles) and MLC-5 (blue circles) plans as a function of maximum effective displacement produced by 0·5º and 1·0º rotations in three directions (roll, pitch, yaw).

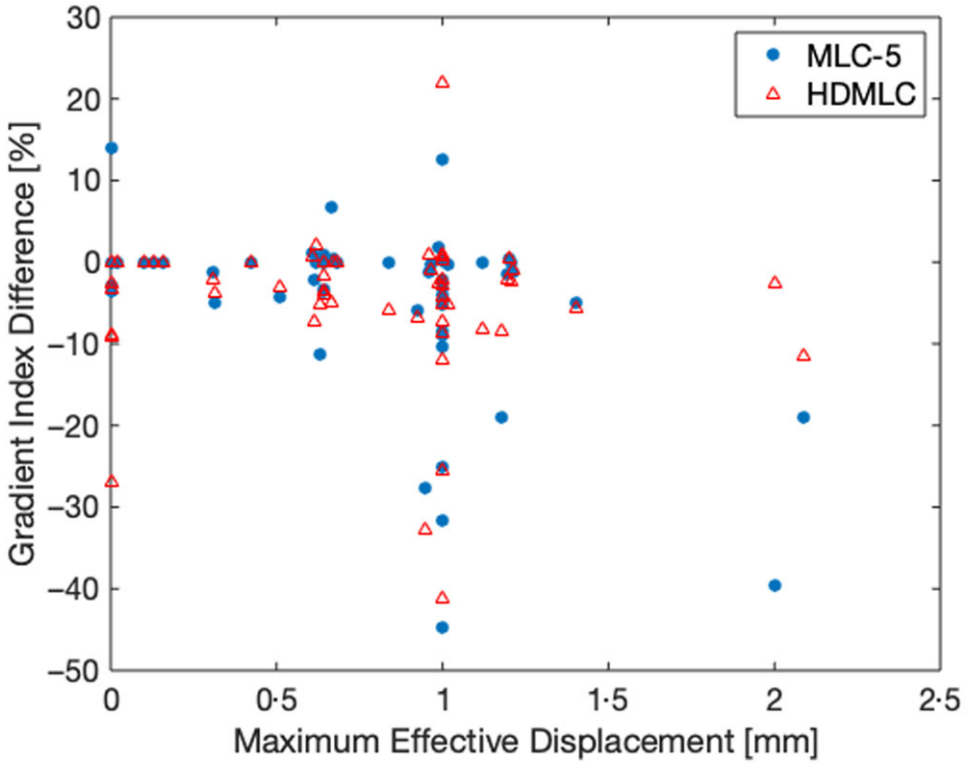


Figure 6. Comparison of the dosimetric difference produced between **rotated** and original plans for gradient index (GI) between the target located in the original position (original) and the displaced (rotated) for HDMLC (red triangles) and MLC-5 (blue circles) plans as a function of maximum effective displacement produced by 0·5º and 1·0º rotations in three directions (roll, pitch, yaw).

https://doi.org/10.1017/S1460396922000048 Published online by Cambridge University Press

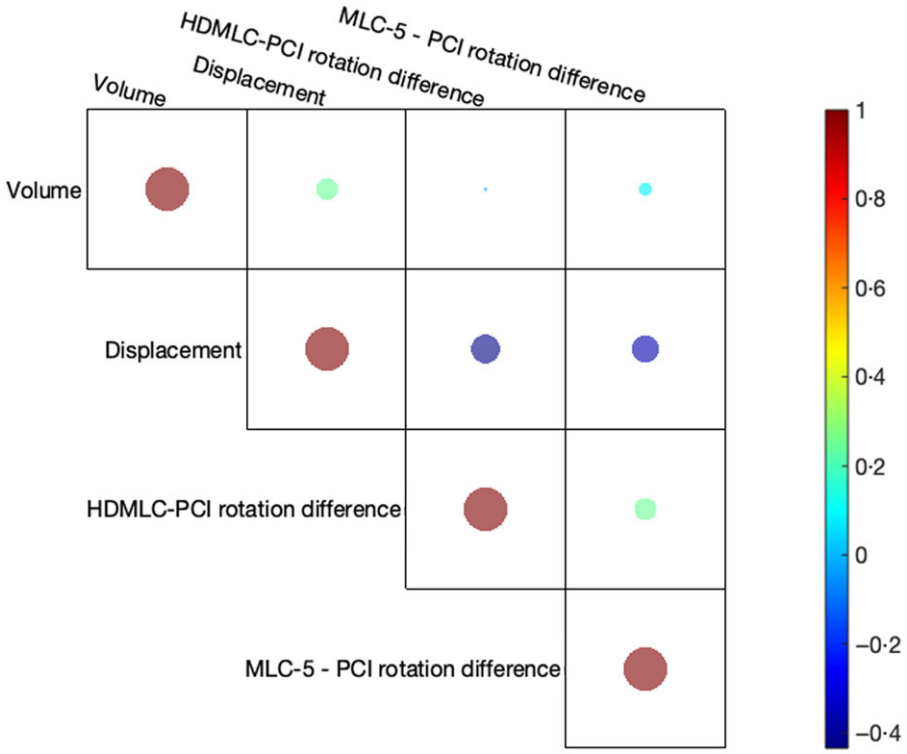


Figure 7. Pearson's correlation coefficients for volume, maximum effective displacement and Paddick conformity index (PCI) dosimetric rotational differences for high-definition multileaf collimator (HDMLC) and MLC-5. The higher the diameter of the circle, the stronger the correlation.

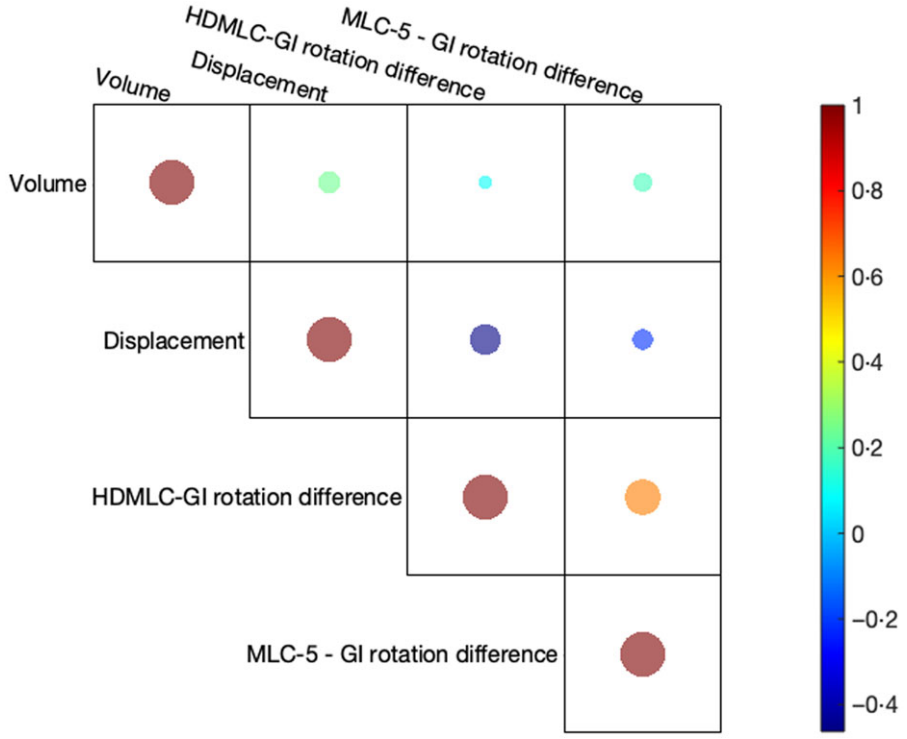


Figure 8. Pearson's correlation coefficients for volume, maximum effective displacement and gradient index (GI) dosimetric rotational differences for high-definition multileaf collimator (HDMLC) and MLC-5. The higher the diameter of the circle, the stronger the correlation.

https://doi.org/10.1017/S1460396922000048 Published online by Cambridge University Press

targets in single isocenter treatments. For normal tissue, mean dose was reduced more effectively by a decrease in MLC width.[19,21]

The most important characteristic in SRS is the precise dose delivery to the target conformally with rapid dose falloff into the surrounding normal tissues. The small positive correlation ($\rho = 0.25$) for PCI rotation-induced dosimetric differences between two types of MLC indicates that it does not depend on the MLC on how closely the radiation prescription dose conforms to the size and shape of the target. In the other hand, there is a high positive correlation ($\rho = 0.62$) for GI that can indicate that the dose falloff outside of the target is dependent on the MLC. The positive correlation shows that there is a directly proportional relation between the dosimetric rotational difference and the displacement produced by rotations. The dosimetric rotational differences for GI are not statistically significant, and the mean values are similar considering their standard deviations (−4% ± 8% for HDMLC and −4% ± 10% for MLC-5).

The use of the institutional PTV margin criterion is necessary for reducing the dosimetric degradation produced by rotations and satisfies the MLC effect on dose coverage, but is not sufficient as reported by past work of our group.[32] Rotational corrections via image guidance are necessary for SRS with a thermoplastic mask for immobilisation. The study of Calmels et al.[29] suggests that patient positioning errors at each couch rotation should be corrected by image guidance systems such as Exactrac® (Brainlab AG, Munchen, Germany). The use of these systems for position correction treatment table avoids compromising dose coverage for metastases located beyond 3 cm from the plan isocenter.[29] There is a clear trade-off between dosimetric quality of small and large targets that should be considered carefully when placing the isocenter.[9,57,58] Regarding the target coverage, there were dosimetric benefits of a finer MLC. However, the downsizing effect of the MLC decreased with the use of a more precise radiotherapy technique and a more sophisticated grade of the same technique.[24,58,59]

The effects of rotational displacements produced for each target in SRS-SIMM are not dependent on the MLC for how closely the dose prescribed conforms to the target but the dose falloff outside of the target is dependent on the MLC. Finer collimator leaves are associated with smaller GI differences with respect to rotational displacements. As described Calmels et al.,[29] PCI close to one is a predictor of local control and sparing of the OAR, while an increase of GI to above three can lead to a higher V_{12} Gy to the healthy brain, which is related to the risk of radionecrosis; therefore, the use of finer collimator leaves considering the rotation-induced displacements in the patient's setup could be associated with a lower risk of necrosis.

The use of GA in SRS offers a novel tool to obtain information concerning the maximum displacement performed by the order and the direction of patient's setup rotations. This fact is valuable, and it can provide well-informed decisions (not only based on geometric concepts) for medical staff to define the appropriate PTV margins. The development of adaptive PTV margins for each metastasis that consider the combined effect of translations, rotations, the dose that healthy brain receive and the specific MLC is proposed as future work.

Conclusion

The finer HDMLC offers dosimetric advantages compared with the MLC-5 in terms of target conformity and dose to the surrounding organs at risk with respect to optimised dynamic arcs from Elements™ Multiple Brain Mts.

The effect of displacements produced by rotations due to setup uncertainties has differentiate effect in both MLC plans for the dose falloff outside of the target. This can be associated with a correct PTV to GTV margins in SIMM-SRS.

Acknowledgements. C. D. Venencia conceived the main idea to the work, planned the treatments, verified the experimental methods and revised the final version to the manuscript.

J. A. Rojas-López performed the computations, developed and verified the in-house software methods, proposed the genetic algorithm optimisation, wrote the manuscript and designed the figures.

R. M. Díaz Moreno processed the DICOM files, developed the in-house software with support from J. A. Rojas-López. R. M. Díaz Moreno revised the final version to the manuscript.

S. Zunino verified and approved the planned treatments, supervised the project and revised the final version to the manuscript.

Financial Support. This research received no specific grant from any funding agency, commercial or not-for-profit sectors.

Conflicts of Interest. Authors declare no conflicts of interest.

Author Agreement. All authors have seen and approved the final version of the manuscript being submitted.

References

1. Brezovich IA, Wu X, Popple RA et al. Stereotactic radiosurgery with MLC-defined arcs: verification of dosimetry, spatial accuracy, and end-to-end tests. J Appl Clin Med Phys 2019; 20 (5): 84–98. doi: 10.1002/acm2.12583
2. Wang SC, Wang X, He YB et al. A dosimetric comparison of the fixed-beam IMRT plans using different leaf width of multileaf collimators for the intermediate risk prostate cancer, Radiat Phys and Chem 2016; 127: 210–221. doi: 10.1016/j.radphyschem.2016.07.008
3. Laoui, S, Kuo JV, Al-Ghazi M, Roa DE. The effect of multileaf collimator leaf width on the quality of volumetric-modulated arc therapy stereotactic radiosurgery treatment plans. Inter J Radiat Oncol Biol Phys 2017; 99 (2): E682–E683. doi: 10.1016/j.ijrobp.2017.06.2248
4. Jin J, Yin F, Ryu S, Ajlouni M, Kim J. Quantitative dosimetric study using different leaf-width multileaf collimators for treatment planning of dynamic conformal and intensity-modulated radiosurgery. Inter J Radiat Oncol Biol Phys 2004; 60 (1): S641. doi: 10.1016/j.ijrobp.2004.07.663
5. Santos T, Ventura T, Capela M, Lopes MC. Dosimetric study on the consequences of replacing the mMLC collimator used for intracranial SRS by an integrated MLC-160. Int J Cancer Clin Res 2016; 3: 064. doi: 10.23937/2378-3419/3/4/1064
6. Kuntz L, Matthis R, Wegner N, Lutz S. Dosimetric comparison of mono-isocentric and multi-isocentric plans for oligobrain metastases: a single institutional experience. Cancer Radiother 2020; 24 (1): 53–59. doi: 10.1016/j.canrad.2019.10.003
7. Slagowski JM, Wen Z. Selection of single-isocenter for multiple-target stereotactic brain radiosurgery to minimize total margin volume. Phys Med Biol 2020; 65 (18): 185012. doi: 10.1088/1361-6560/ab9703
8. Nakano H, Tanabe S, Utsunomiya S et al. Effect of setup error in the single-isocenter technique on stereotactic radiosurgery for multiple brain metastases. J Appl Clin Med Phys 2020; 21–12:155–165. doi: 10.1002/acm2.13081
9. Stanhope C, Chang Z, Wang Z et al. Physics considerations for single-isocenter, volumetric modulated arc radiosurgery for treatment of multiple intracranial targets. Pract Radiat Oncol 2016; 6 (3): 207–213. doi: 10.1016/j.prro.2015.10.010
10. Kraft J, van Timmeren JE, Mayinger M et al. Distance to isocenter is not associated with an increased risk for local failure in LINAC-based single-isocenter SRS or SRT for multiple brain metastases. Radiother Oncol 2021; 159: 168–175. doi: 10.1016/j.radonc.2021.03.022
11. Prentou G, Pappas EP, Logothetis A et al. Dosimetric impact of rotational errors on the quality of VMAT-SRS for multiple brain metastases:

comparison between single- and two-isocenter treatment planning techniques. J Appl Clin Med Phys 2020; 21 (3): 32–44. doi: 10.1002/acm2.12815
12. Roper J, Chanyavanich V, Betzel G, Switchenko J, Dhabaan A. Single-isocenter multiple-target SRS: risk of compromised coverage. Int J Radiat Oncol Biol Phys 2015; 93 (3): 540–546. doi: 10.1016/j.ijrobp.2015.07.2262
13. Ruggieri R, Naccarato S, Mazzola R et al. Linac-based VMAT radiosurgery for multiple brain lesions: comparison between a conventional multi-isocenter approach and a new dedicated mono-isocenter technique. Radiat Oncol 2018; 13: 38. doi: 10.1186/s13014-018-0985-2
14. Bortfeld T, Schlegel W, Höver KH, Schulz-Ertner D, Mini and micro multileaf collimators. German Cancer Research Center (DKFZ). https://www.aapm.org/meetings/99AM/pdf/2796-50260.pdf, Accesed July 19, 2021.
15. Wu QJ, Wang Z, Kirkpatrick JP et al. Impact of collimator leaf width and treatment technique on stereotactic radiosurgery and radiotherapy plans for intra- and extracranial lesions. Radiat Oncol 2009; 4: 3. doi: 10.1186/1748-717X-4-3
16. Bossart E, Mellon EA, Monterroso I et al. Assessment of single isocenter linear accelerator radiosurgery for metastases and base of skull lesions. Phys Med 2021; 81: 1–8. doi: 10.1016/j.ejmp.2020.11.011
17. Monk JE, Perks JR, Doughty D, Plowman PN. Comparison of a micro-multileaf collimator with a 5-mm-leaf-width collimator for intracranial stereotactic radiotherapy. Int J Radiat Oncol Biol Phys 2003; 57: 1443–1449. doi: 10.1016/s0360-3016(03)01579-7
18. Chern SS, Leavitt DD, Jensen RL, Shrieve DC. Is smaller better? Comparison of 3-mm and 5-mm leaf size for stereotactic radiosurgery: A dosimetric study. Int J Radiat Oncol Biol Phys 2006; 66: 76–81. doi: 10.1016/j.ijrobp.2006.04.061
19. Jin JY, Yin FF, Ryu S, Ajlouni M, Kim JH. Dosimetric study using different leaf-width MLCs for treatment planning of dynamic conformal arcs and intensity modulated radiosurgery. Med Phys 2005; 32: 405–411. doi: 10.1118/1.1842911
20. Kubo HD, Wilder RB, Pappas CTE. Impact of collimator leaf width on stereotactic radiosurgery and 3D conformal radiotherapy treatment plans. Int J Radiat Oncol Biol Phys 1999; 44: 937–945. doi: 10.1016/S0360-3016(99)00041-3
21. Burmeister J, McDermott PN, Bossenberger T et al. Effect of MLC leaf width on the planning and delivery of SMLC IMRT using the CORVUS inverse treatment planning system. Med Phys 2004; 31: 3187–3193. doi: 10.1118/1.1812607
22. Tanyi JA, Kato CN, Chen Y, Chen Z, Fuss M. Impact of the high definition multileaf collimator on linear accelerator-based intracranial stereotactic radiosurgery. Br J Radiol 2011; 84: 629–638. doi: 10.1259/bjr/19726857
23. Marrazzo L, Zani M, Pallotta S et al. Comparison of stereotactic plans for brain tumors with two different multileaf collimating systems. J Appl Clin Med Phys 2014; 15: 27–37. doi: 10.1120/jacmp.v15i1.4100
24. Abisheva Z, Floyd SR, Salama JK et al. The effect of MLC leaf width in single-isocenter multi-target radiosurgery with volumetric modulated arc therapy. J Radiosurg SBRT 2019; 6 (2): 131–138. https://pubmed.ncbi.nlm.nih.gov/31641549. Accessed March 20, 2021.
25. Tsui SSW, Wu VWC, Cheung JSC. Comparison of dosimetric impact of intra-fractional setup discrepancy between multiple- and single-isocenter approaches in linac-based stereotactic radiotherapy of multiple brain metastases. J Appl Clin Med Phys 2021. doi: 10.1002/acm2.13484
26. Klein EE, Hanley J, Bayouth J et al. Task Group 142 report: quality assurance of medical accelerators. Med Phys 2009; 36 (9): 4197–212. doi: 10.1118/1.3190392
27. Lutz W, Winston KR, Maleki N. A system for stereotactic radiosurgery with a linear accelerator. Int J Radiat Oncol Biol Phys 1988; 14 (2): 373–381. doi: 10.1016/0360-3016(88)90446-4
28. Kim S, Tseng TC, Morrow A. Spatial variations of multiple off-axial targets for a single isocenter SRS treatment in Novalis Tx linac system. J Radiosurg SBRT 2015; 3 (4): 287–296.
29. Calmels L, Blak Nyrup Biancardo S, Sibolt P et al. Single-isocenter stereotactic non-coplanar arc treatment of 200 patients with brain metastases: multileaf collimator size and setup uncertainties. Strahlenther Onkol 2021. doi: 10.1007/s00066-021-01846-6
30. Zhou S, Li J, Du Y, Yu S, Wang M, Wu H, Yue H. Development and longitudinal analysis of plan-based streamlined quality assurance on multiple positioning guidance systems with single phantom setup. Front Oncol 2021; 11: 683733. doi: 10.3389/fonc.2021.683733
31. Molinier J, Kerr C, Simeon S, Ailleres N, Charissoux M, Azria D, Fenoglietto P. Comparison of volumetric-modulated arc therapy and dynamic conformal arc treatment planning for cranial stereotactic radiosurgery. J Appl Clin Med Phys 2016; 17 (1): 92–101. doi: 10.1120/jacmp.v17i1.5677
32. Rojas-López JA, Díaz Moreno RM, Venencia CD. Use of genetic algorithm for PTV optimization in single isocenter multiple metastases radiosurgery treatments with Brainlab Elements™. Phys Med 2021; 86: 82–90. doi: 10.1016/j.ejmp.2021.05.031
33. Ezzell GA. The spatial accuracy of two frameless, linear accelerator-based systems for single-isocenter, multitarget cranial radiosurgery. J Appl Clin Med Phys 2017; 18: 37–43. doi: 10.1002/acm2.12044
34. Guckenberger M, Roesch J, Baier K, Sweenwy RA, Flentje M. Dosimetric consequences of translational and rotational errors in frame-less image-guided radiosurgery. Radiat Oncol 2012; 63–67. doi: 10.1186/1748-717X-7-63
35. Jhaveri J, Chowdhary M, Zhang X et al. Does size matter? Investigating the optimal planning target volume margin for postoperative stereotactic radiosurgery to resected brain metastases. J Neurosurg 2018; 130 (3): 797–803. doi: 10.3171/2017.9.JNS171735
36. Vergalasova I, Liu H, Alonso-Basanta M et al. Multi-institutional dosimetric evaluation of modern day Stereotactic Radiosurgery (SRS) treatment options for multiple brain metastases. Front. Oncol 2019; 9: 483. doi: 10.3389/fonc.2019.00483
37. Gevaert T, Steenbeke F, Pellegri L et al. Evaluation of a dedicated brain metastases treatment planning optimization for radiosurgery: a new treatment paradigm? Radiat Oncol 2016: 11–13. doi: 10.1186/s13014-016-0593-y
38. Medical Physics. Institute of radiooncology, KFJ Hospital Vienna. Dosimetric Parameters of the HD120 MLC. https://www.wienkav.at/kav/kfj/91033454/physik/irohome.html. Accessed July 7, 2021.
39. TrueBeam technical reference guide: Volumen 2 -Imaging P-005924002-B, Varian Medical System. 2016. https://www.wienkav.at/kav/kfj/91033454/physik/irohome.htm. Accessed September 10, 2021.
40. Sharma DS, Dongre PM, Mhatre V, Heigrujam M. Physical and dosimetric characteristic of high-definition multileaf collimator (HDMLC) for SRS and IMRT. J Appl Clin Med Phys 2011; 12 (3): 3475. doi: 10.1120/jacmp.v12i3.3475
41. Mohan R, Chui C, Lidofsky L. Energy and angular distributions of photons from medical linear accelerators. Med Phys 1985; 12 (5): 592–597. doi: 10.1118/1.595680
42. Mohan R, Chui C, Lidofsky L. Differential pencil beam dose computation model for photons. Med Phys 1986; 13 (1): 64–73. doi: 10.1118/1.595924
43. Mohan R, Chui CS. Use of fast Fourier transforms in calculating dose distributions for irregularly shaped fields for three-dimensional treatment planning. Med Phys 1987; 14 (1): 70–77. doi: 10.1118/1.596097
44. Rojas-López JA, Venencia CD. Importance of Beam-Matching between TrueBeam STx and Novalis Tx in Pre-treatment quality assurance using portal dosimetry. J Med Phys 2021; 46: 211–220. doi: 10.4103/jmp.JMP_12_21
45. Paddick I. A simple scoring ratio to index the conformity of radiosurgical treatment plans. Technical note. J Neurosurg 2000; 93 (Suppl 3): 219–232. doi: 10.3171/jns.2000.93.supplement
46. Paddick I, Lippitz B. A simple dose gradient measurement tool to complement the conformity index. J Neurosurg (Suppl) 2006; 105: 194–201. doi: 10.3171/sup.2006.105.7.194
47. Balagamwala EH, Suh JH, Barnett GH et al. The importance of the conformality, heterogeneity, and gradient indices in evaluating gamma knife radiosurgery treatment plans for intracranial meningiomas. Int J Radiat Oncol Biol Phys 2012; 83 (1): 1406–1413. doi: 10.1016/j.ijrobp.2011.10.024
48. Wagner TH, Bova FJ, Friedman WA, Buatti JM, Bouchet LG, Meeks SL. A simple and reliable index for scoring rival stereotactic radiosurgery plans.

https://doi.org/10.1017/S1460396922000048 Published online by Cambridge University Press

Int J Radiat Oncol Biol Phys 2003; 57 (4): 1141–1149. doi: 10.1016/s0360-3016(03)01563-3
49. Sale M, Sherer EA. A genetic algorithm based global search strategy for population pharmacokinetic/pharmacodynamic model selection. Br J Clin Pharmacol 2015; 79 (1): 28–39. doi: 10.1111/bcp.12179
50. Shi X, Long W, Li Y, Deng D. Multi-population genetic algorithm with ER network for solving flexible job shop scheduling problems. PLoS One 2020; 15 (5): e0233759. doi: 10.1371/journal.pone.0233759
51. Ghosh M, Adhikary S, Ghosh KK, Sardar A, Begum S, Sarkar R. Genetic algorithm based cancerous gene identification from microarray data using ensemble of filter methods. Med Biol Eng Comput 2019; 57 (1): 159–176. doi: 10.1007/s11517-018-1874-4
52. Mantzaris D, Anastassopoulos G, Adamopoulos A. Genetic algorithm pruning of probabilistic neural networks in medical disease estimation. Neural Netw 2011; 24 (8): 831–835. doi: 10.1016/j.neunet.2011.06.003
53. Geng X, Guan J, Dong Q, Zhou S. An improved genetic algorithm for statistical potential function design and protein structure prediction. Int J Data Min Bioinform 2012; 6 (2): 162–177. doi: 10.1504/ijdmb.2012.048174
54. Huang Y, Chin K, Robbins JR et al. Radiosurgery of multiple brain metastases with single-isocenter dynamic conformal arcs (SIDCA). Radiother Oncol 2014; 112 (1): 128–132. doi: 10.1016/j.radonc.2014.05.009
55. Clark GM, Popple RA, Young PE, Fiveash JB. Feasibility of single-isocenter volumetric modulated arc radiosurgery for treatment of multiple brain metastases. Int J Radiat Oncol Biol Phys 2010; 76 (1): 296–302. doi: 10.1016/j.ijrobp.2009.05.029
56. Novalis Circle Symposium. Impact of margins for single isocenter multiple target treatments AAPM 2019. https://www.novaliscircle.org/video/impact-of-margins-for-single-isocenter-multiple-target-treatments-dWQSM9a/. Accessed October 8, 2020.
57. Chae S, Woong LK, Hyun S S. Dosimetric impact of multileaf collimator leaf width according to sophisticated grade of technique in the IMRT and VMAT planning for pituitary adenoma lesion. Oncotarget 2016; 7: 78119–78126. Retrieved from https://www.oncotarget.com/article/12974/text/. Accessed July 21, 2021.
58. Shaw E, Kline R, Gillin M et al. Radiation therapy oncology group: radiosurgery quality assurance guidelines. Int J Radiat Oncol Biol Phys, 1993; 27 (5): 1231–1239. doi: 10.1016/0360-3016(93)90548-a
59. Ohtakara K, Hayashi S, Tanaka H, Hoshi H. Dosimetric comparison of 2.5 mm vs. 3.0 mm leaf width micro-multileaf collimator-based treatment systems for intracranial stereotactic radiosurgery using dynamic conformal arcs: implications for treatment planning. Jpn J Radiol 2011; 29 (9): 630–638. doi: 10.1007/s11604-011-0606-6

https://doi.org/10.1017/S1460396922000048 Published online by Cambridge University Press